International Tables for Crystallography (2006). Vol. F, Chapter 11.5, pp. 236–245.

11.5. The use of partially recorded reflections for post refinement, scaling and averaging X-ray diffraction data

BY C. G. VAN BEEK, R. BOLOTOVSKY AND M. G. ROSSMANN

11.5.1. Introduction

Recent advances in the use of frozen crystals of biological samples for X-ray diffraction data collection (Rodgers, 1994) often result in data for which most of the observed reflections on each frame are partially observed. This might be avoided by increasing the oscillation ranges, but this would cause many reflections to overlap with their neighbours. Hence, it is necessary to develop scaling procedures that are independent of the exclusive use of fully recorded reflections.

A set of measured Bragg intensities is dependent on the properties of the crystal, radiation source and detector. Usually, these factors cannot be kept constant throughout the data collection. The crystal may decay, weakening the Bragg intensities, or even 'die', which requires the use of several crystals for a full data set. The intensity and position of the primary X-ray beam may vary, especially at synchrotron-radiation sources. Finally, the detector response may change when, for example, different films or imaging plates are used during the data collection.

Most data sets can be divided into series of subsets, or frames, collected under more-or-less constant conditions. These frames need to be placed on a common arbitrary scale. The scaling can be performed by comparing the intensities of multiply measured reflections or symmetry-equivalent reflections on different frames.

A least-squares procedure frequently used for scaling frames of data is the Hamilton, Rollett and Sparks (HRS) method (Hamilton *et al.*, 1965). The target for the HRS least-squares minimization is

$$\psi = \sum_h \sum_i W_{hi}(I_{hi} - G_m I_h)^2, \qquad (11.5.1.1)$$

where I_h is the best estimate of the intensity of a reflection with reduced Miller indices h, I_{hi} is the intensity of the ith measurement of reflection h, W_{hi} is a weight for reflection h_i and G_m is the inverse linear scale factor for frame m on which reflection h_i is recorded. The reduced Miller indices are those corresponding to an arbitrarily defined asymmetric unit of reciprocal space. The HRS expression (11.5.1.1) assumes that all reflections h_i are full, that is, their reciprocal-lattice points have completely passed through the Ewald sphere.

For all unique reflections h, the values of I_h must correspond to a minimum in ψ. Thus,

$$\partial\psi/\partial I_h = 0. \qquad (11.5.1.2)$$

Therefore, the best least-squares estimate of the intensity of a reflection is

$$I_h = \sum_i W_{hi} G_m I_{hi} \Big/ \sum_i W_{hi} G_m^2. \qquad (11.5.1.3)$$

Since ψ is not linear with respect to the scale factors G_m, the values of the scale factors have to be determined by an iterative nonlinear least-squares procedure. As the scale factors are relative to each other, the HRS procedure requires that one of them be fixed.

Fox & Holmes (1966) describe an improved method of solving the HRS normal equations. Their approach is based on the singular value decomposition of the normal equations matrix. The advantage of the Fox and Holmes method, apart from the accelerated convergence of the least-squares procedure, is that no *ad hoc* decision needs to be made as to which scale factor should be fixed. Furthermore, 'troublesome' frames of data can be identified as causing negligibly small eigenvalues in the normal equations matrix.

11.5.2. Generalization of the Hamilton, Rollett and Sparks equations to take into account partial reflections

When a Bragg reflection is completely exposed within the oscillation range of one frame, a so-called 'full reflection', it gives rise to the 'full intensity'. In general, a Bragg reflection will occur on a number of consecutive frames as a series of partial reflections, and the full intensity can only be estimated from the measured intensities of the partial reflections. Let I_{him} represent the intensity contribution of reflection h_i recorded on frame m; if all the parts of h_i are available in the data set, then

$$I_{hi} = \sum_m (I_{him}/G_m). \qquad (11.5.2.1)$$

In practice, there will always be reflections that do not have all their parts available. In such cases, the only way to estimate the full intensity of a reflection is to apply an estimated value of the partiality to the measured reflection intensities.

Various models have been proposed to calculate the reflection partiality. Here we use Rossmann's model (Rossmann, 1979; Rossmann *et al.*, 1979) with Greenhough & Helliwell's (1982) correction. This model treats partiality as a fraction of a spherical volume swept through the Ewald sphere. The coordinates of the reciprocal-lattice point are defined by the Miller indices of the reflection, the crystal orientation matrix and the rotation angle. The volume of the sphere around the reciprocal-lattice point accounts for crystal mosaicity and beam divergence. Alternative geometrical descriptions of a reciprocal-lattice point passing through the Ewald sphere have been given by Winkler *et al.* (1979) and Bolotovsky & Coppens (1997).

Provided the reflection partiality, p_{him}, is known, the full intensity is estimated by

$$I_{hi} = I_{him}/p_{him}G_m. \qquad (11.5.2.2)$$

This expression can produce as many estimates of I_{hi} as there are parts of reflection h_i, while expression (11.5.2.1) produces only one estimate of I_{hi} when all parts of reflection h_i are recorded. Having defined the relationships between measured intensities of partial reflections and estimated full reflections by expressions (11.5.2.1) and (11.5.2.2), two methods of generalizing the HRS equations can be considered.

Method 1. If a reflection h_i occurs on a number of consecutive frames and all parts of I_{him} are available in the data set, the generalized HRS target equation takes the form

$$\psi = \sum_h \sum_i \sum_m W_{him} \left\{ I_{him} - G_m \left[I_h - \sum_{m' \neq m} (I_{him'}/G_{m'}) \right] \right\}^2. \qquad (11.5.2.3)$$

Using expression (11.5.1.2), the best least-squares estimate of I_h will be

$$I_h = \frac{\sum_i \left[\sum_m (I_{him}/G_m)\right]\left(\sum_m W_{him} G_m^2\right)}{\sum_i \sum_m W_{him} G_m^2} = \frac{\sum_i I_{hi} \sum_m W_{him} G_m^2}{\sum_i \sum_m W_{him} G_m^2}. \qquad (11.5.2.4)$$

Method 2. If the theoretical partiality, p_{him}, of the partially recorded reflection h_{im} can be estimated, the generalized HRS target equation takes the form

$$\psi = \sum_h \sum_i \sum_m W_{him}(I_{him} - G_m p_{him} I_h)^2 \qquad (11.5.2.5)$$

and, using expression (11.5.1.2), the best least-squares estimate of I_h will then be

$$I_h = \frac{\sum_i \sum_m W_{him} G_m p_{him} I_{him}}{\sum_i \sum_m W_{him} G_m^2 p_{him}^2}. \qquad (11.5.2.6)$$

When all reflections in the data set are fully recorded, expressions (11.5.2.3) and (11.5.2.5) reduce to the 'classical' HRS expression (11.5.1.1), and expressions (11.5.2.4) and (11.5.2.6) reduce to expression (11.5.1.3).

The scale factor G_m can be generalized to incorporate crystal decay (Gewirth, 1996; Otwinowski & Minor, 1997):

$$G_{him} = G_m \exp\left\{-2B_m[\sin(\theta_{hi})/\lambda]^2\right\}, \qquad (11.5.2.7)$$

where B_m is a parameter describing the crystal disorder while frame m was recorded, θ_{hi} is the Bragg angle of reflection h_i and λ is the X-ray wavelength.

Method 1 only allows the refinement of the scale factors while method 2 allows refinement of the scale factors, crystal mosaicity and orientation matrix, as the latter two factors contribute to the calculated partiality. Furthermore, method 2 is essential for scaling of data sets with low redundancy (*e.g.* data collected from low-symmetry crystals or data collected over small rotation ranges). When a reflection h_i spans more than one frame, but there are no other reflections with the same reduced Miller indices h in the data set, the contribution of any partial reflection h_{im} to expression (11.5.2.3) will be zero, as in this case I_h will be the same as I_{hi}. In contrast, in method 2 the reflection h_i can be used for scaling because the estimates of the full intensity I_{hi} are calculated independently from every frame spanned by reflection h_i.

11.5.3. Selection of reflections useful for scaling

Both scaling methods 1 and 2 may take into account any reflection intensity observation, regardless of whether it is a partially or fully recorded reflection. However, there are significant differences between the selection of reflections in the two methods. Method 1 requires that all parts of a reflection are available in order to incorporate the reflection into the generalized HRS target, expression (11.5.2.3). Thus, reflections that occur at the beginning or the end of the crystal orientation, or at gaps within the rotation range, must be rejected. Even when all parts of a reflection are recorded, there might be parts for which there was a problem during integration, thus making the reflection useless for scaling. The decision on whether all parts of a reflection are available for scaling is dependent on knowledge of the crystal mosaicity and of the crystal orientation matrix. Since these might be inaccurate, a reasonable tolerance has to be exercised when deciding if a reflection has been completely measured on consecutive frames. Method 2 allows the use of all reflections for scaling as every observation of a partial reflection is sufficient to estimate the intensity of a full reflection, expression (11.5.2.2). However, a reasonable lower limit of calculated partiality has to be imposed in selecting reflections useful for scaling. The criteria for rejecting reflections prior to scaling and averaging are listed in Table 11.5.3.1.

11.5.4. Restraints and constraints

Scale factors will depend on the variation of the incident X-ray beam intensity, crystal absorption and radiation damage. Hence, in general, scale factors can be constrained to follow an analytical function or restrained to minimize variation between successive frames. The scale factors can be restrained by adding a term $w(G_n - G_{n+1})^2$ to ψ, expression (11.5.1.1), where G_n and G_{n+1} are scale factors for the nth and $(n+1)$th frame and w is a suitably chosen weight. Such procedures will increase $R_{\rm merge}$ but will also increase the accuracy of the scaled intensities as additional reasonable physical conditions have been applied.

The mis-setting angles of a single crystal should remain constant throughout the data set. Thus, in principle, the mis-setting angles should be constrained to be the same for all frames associated with a single crystal in the data set. However, in practice, independent refinement of the mis-setting angles can detect problems in the data set when there are discontinuities in these angles with respect to frame number. Cell dimensions should be the same for all crystals and might therefore be constrained. However, care should be taken, as the exact conditions of freezing may cause some variations in cell dimensions between crystals. As radiation damage proceeds, mosaicity is likely to increase. Hence, constraint between the refined mosaicities of neighbouring frames can be useful.

Table 11.5.3.1. *Hierarchy of criteria for selecting reflections for scaling and averaging procedures*

Methods 1 and 2	
All parts of a reflection are rejected if: (1) There are no successfully integrated parts. (2) There are no parts with significant intensity (for scaling only). (3) There are some parts entering and some parts exiting the Ewald sphere (this implies that the reflection is too close to the rotation axis and is partly in the blind zone). (4) This is a full reflection recorded only once with no other symmetry-equivalent observations.	
Method 1	Method 2
All parts of a reflection are rejected if: (1) There is a part that is not successfully integrated. (2) There is a part that has a significant intensity, but is not predicted by the crystal orientation and mosaicity used in the scaling program. (3) The sum of calculated partialities differs from unity by more than a chosen value.	Any part of a reflection is rejected if: (1) The calculated partiality is less than a chosen value. (2) The intensity is less than a chosen fraction of the error estimate.

11.5.5. Generalization of the procedure for averaging reflection intensities

Once the scale factors of all frames are determined, they need to be applied to the reflection intensities and error estimates. The reflection intensities with the same reduced Miller indices can then be averaged.

When method 2 is used for averaging, the determination of $\langle I_h \rangle$ is more complicated as there are as many estimates of the full intensity I_{hi} as there are partial reflections h_{im}. Therefore, intensity averaging of reflection h has to be done in two steps. First, for every reflection h_i, the intensity estimates from all partial observations will be the weighted mean, where the weights are based on the estimated standard deviations of each intensity measurement. In the second step, the average is taken over the i different scaled intensities for the observed reflections.

The selection of reflections useful for averaging is the same as for scaling (Table 11.5.3.1), except that it is no longer necessary to reject reflections that have insignificant intensities. Applying a σ cutoff while averaging the scaled intensities will lead to a statistical bias of the weaker reflection intensities.

For samples of three or more equivalent reflections, it is necessary to consider the absolute values of the differences between individual intensities and the median of the sample: $|I_{hi} - I_{\rm median}|$. The outliers can be detected by several statistical tests and, once detected, can be either down-weighted or rejected. When the sample consists of only two reflections, they can be considered a 'discordant pair' if the difference between their intensities is not warranted by the estimated errors and, hence, both reflections can be rejected (Blessing, 1997).

Averaging intensities estimated according to method 2 has an advantage over method 1 as outliers and discordant pairs can be 'screened' at two levels: firstly, when the estimates of the full reflection intensity I_{hi}, calculated by expression (11.5.2.2) from different parts of the same reflection, are considered, and secondly when the mean intensities $\langle I_{hi} \rangle$ from different reflections are considered.

11.5.6. Estimating the quality of data scaling and averaging

A commonly used estimate of the quality of scaled and averaged Bragg reflection intensities is $R_{\rm merge}$. Useful definitions of R factors are:

$$R_{\rm merge} = \quad R_1 = \left[\left(\sum_h \sum_i |I_{hi} - \langle I_h \rangle| \right) \Big/ \sum_h \sum_i |I_{hi}| \right] \times 100\%, \tag{11.5.6.1}$$

$$R_2 = \left\{ \left[\sum_h \sum_i (I_{hi} - \langle I_h \rangle)^2 \right] \Big/ \sum_h \sum_i I_{hi}^2 \right\} \times 100\% \tag{11.5.6.2}$$

$$\text{and} \quad R_w = \left\{ \left[\sum_h \sum_i W_{hi} (I_{hi} - \langle I_h \rangle)^2 \right] \Big/ \sum_h \sum_i W_{hi} I_{hi}^2 \right\} \times 100\%. \tag{11.5.6.3}$$

The linear (R_1), square (R_2) and weighted (R_w) R factors can be subdivided into resolution ranges, intensity ranges, reflection classes, frame number and regions of the detector surface. When method 1 is used, reflections h_i can be grouped in terms of the sums of partialities of contributing partial reflections h_{im}.

The R-factor variation depends on the properties of the detector with respect to intensities. Generally the R factor decreases as intensity increases. Thus, the R factor generally increases with resolution. Any deviation from this behaviour might indicate a problem in the data collection due to nonlinearity of the detector response, ice diffuse diffraction, or any other stray effects superimposed on the crystal diffraction.

A useful indicator of the quality of the intensity estimates of partial reflections is the mean ratio of calculated partiality to observed partiality:

$$r_p = \langle p_{him}^{\rm calc} / p_{him}^{\rm obs} \rangle = \langle p_{him}^{\rm calc} \langle I_h \rangle / I_{him} \rangle. \tag{11.5.6.4}$$

The deviation of this ratio from unity can be examined as a function of the reflection intensity, resolution and calculated partiality.

The comparison of R factors for centric and noncentric reflections can be used to determine the significance of an anomalous-scattering effect. The quality of the anomalous-dispersion signal can be assessed by calculation of the scatter, σ_{Ih}, where

$$\sigma_{Ih} = \left\{ \left[1/(n-1) \right] \sum_n (\langle I_h \rangle - I_{hn})^2 \right\}^{1/2} \tag{11.5.6.5}$$

and $\langle I_h \rangle$ is the average of the n measurements of the full reflection intensities I_{hn}. The σ_{Ih} values for noncentric reflections can be compared to the scatter, σ_{Ih}^+ or σ_{Ih}^-, of reflections differing only in absorption while excluding Bijvoet opposites. The mean scatter is calculated from all σ_{Ih} values,

$$\langle \sigma_{Ih} \rangle = (1/h) \sum_h \left\{ \left[1/(n-1) \right] \sum_n (\langle I_h \rangle - I_{hn})^2 \right\}^{1/2}. \tag{11.5.6.6}$$

The ratios $\langle \sigma_{Ih} \rangle / \langle \sigma_{Ih}^+ \rangle$ and $\langle \sigma_{Ih} \rangle / \langle \sigma_{Ih}^- \rangle$ should be larger than unity for significant anomalous-dispersion data.

11.5.7. Experimental results

11.5.7.1. *Variation of scale factors versus frame number*

If scale factors are to make physical sense, their behaviour with respect to the frame number has to be in accordance with the known changes in the beam intensity, crystal condition and detector response.

The scaling of a φX174 procapsid data set (Dokland *et al.*, 1997) was performed using methods 1 and 2 as described here and using *SCALEPACK* (Otwinowski & Minor, 1997) (Fig. 11.5.7.1). Graphs (*a*) and (*b*) in Fig. 11.5.7.1 have four segments corresponding to four synchrotron beam 'fills'. All three methods give scale factors within 5% of each other (Figs. 11.5.7.1*c* and *d*). However, for the first and last frame of each 'fill' the results can differ by as much as 15%. Both method 1 and *SCALEPACK* produce physically wrong results in that the scale factors of these frames look like outliers compared to the scale factors of the neighbouring frames. By contrast, method 2 provides consistent scale factors for these frames. Although the algorithm used by *SCALEPACK* for scaling frames with partial reflections has never been disclosed, the similar results obtained by method 1 and *SCALEPACK* suggest that *SCALEPACK* might be using an algorithm similar to that of method 1 (Fig. 11.5.7.1*d*).

Attempts at scaling a data set of a frozen crystal of HRV14 (Rossmann *et al.*, 1985, 1997) failed with method 1 as a result of gaps in the rotation range for the first 20 frames, causing singularity of the normal equations matrix. When frames without useful neighbours were excluded, the cubic symmetry of the crystal was sufficient for successful scaling. In contrast, method 2 did not have any problems with the whole data set, and the results obtained with method 2 showed greater consistency than those obtained with method 1 or *SCALEPACK* (Fig. 11.5.7.2).

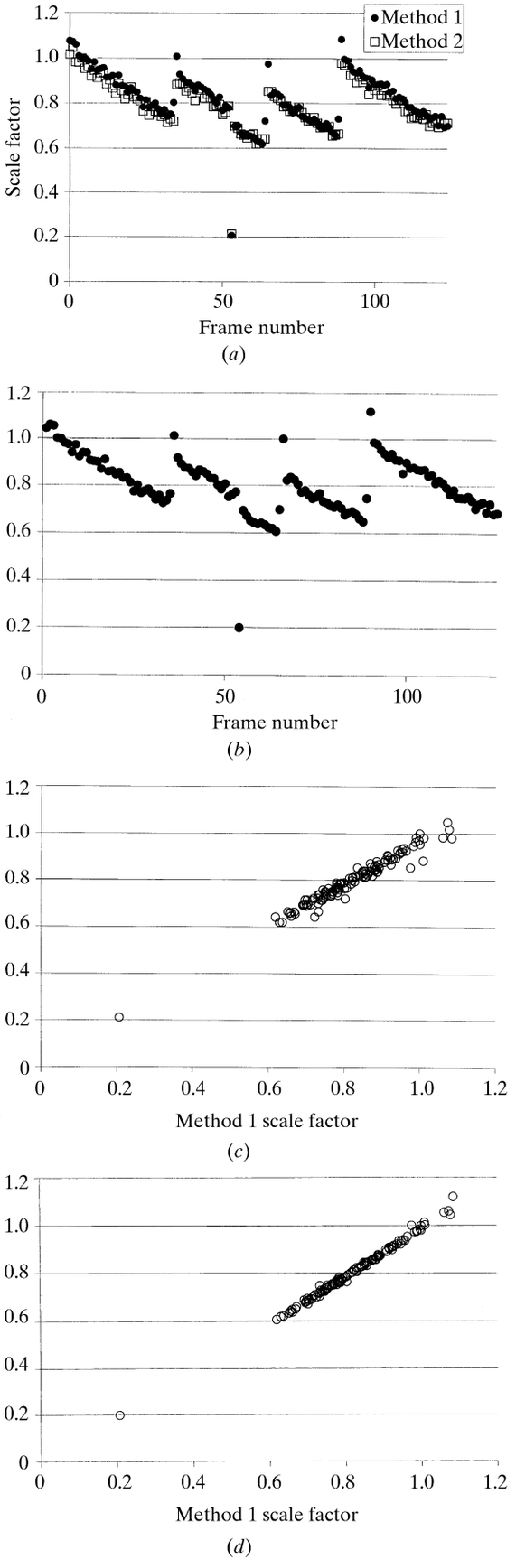

Fig. 11.5.7.1. Linear scale factors as a function of frame number for a φX174 data set (Dokland *et al.*, 1997). Results from (*a*) method 1 and method 2, (*b*) *SCALEPACK*. Comparison of (*c*) method 2 *versus* method 1, and (*d*) *SCALEPACK versus* method 1.

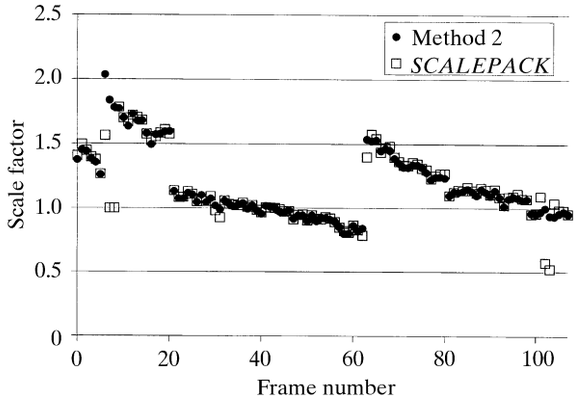

Fig. 11.5.7.2. Linear scale factor as a function of frame number for an HRV14 data set (Rossmann *et al.*, 1985, 1997).

The accuracy and robustness of method 2 is also demonstrated by the scaling results for a Sindbis virus capsid protein (SCP), residues 114–264 (Choi *et al.*, 1991, 1996). The behaviour of the scale factor with respect to the frame number reflects the anisotropy of the thin plate-shaped crystal (Fig. 11.5.7.3). For the first 40 frames (frame numbers 0 to 39), even-numbered frames have higher scale factors than odd-numbered frames. Data collection was stopped after frame number 39 and restarted. After frame number 39, odd-numbered frames have higher scale factors than even-numbered frames. This effect presumably relates to the use of the two alternating image plates with slightly different sensitivities in the *R*-axis camera used in the data collection.

11.5.7.2. *R factor as a function of 'sum-of-partialities' (method 1)*

In order to determine the limits of tolerance that can be permitted when method 1 is used, the *R* factor was examined as a function of the sum-of-partialities for the φX174 procapsid data (Fig. 11.5.7.4). Reflections with sum-of-partialities of 1 ± 0.3 were used. The *R* factor changes sharply when the sum-of-partialities is outside 1 ± 0.15. Hence, ± 0.15 were acceptable limits of tolerance for this data set.

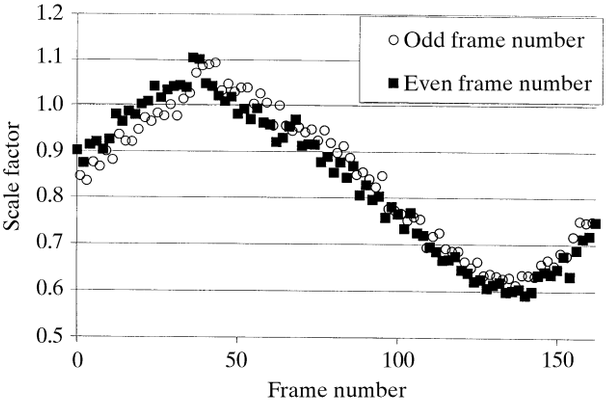

Fig. 11.5.7.3. Linear scale factor determined by method 2 as a function of frame number for an SCP(114–264) data set (Choi *et al.*, 1991, 1996). The sine-like pattern reflects the anisotropy of a thin plate-shaped crystal.

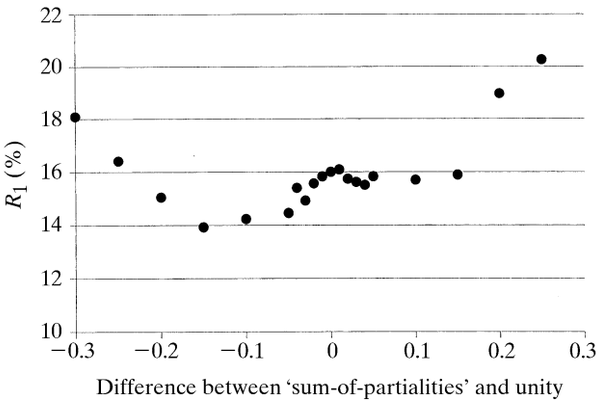

Fig. 11.5.7.4. *R* factor as a function of the difference of calculated 'sum-of-partialities' and unity for the estimates of full reflections when method 1 is used for the scaling and averaging of a φX174 data set (Dokland *et al.*, 1997).

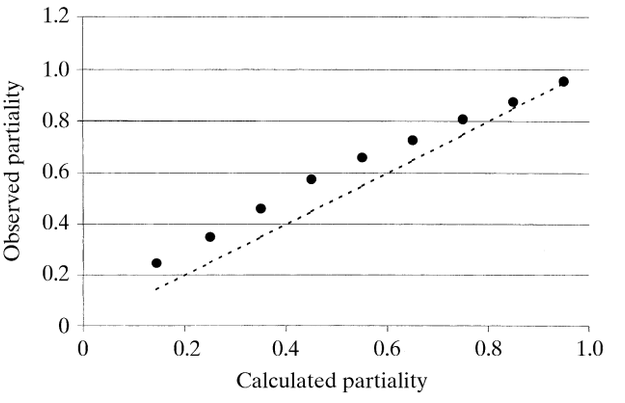

Fig. 11.5.7.6. The observed partialities plotted against calculated partialities for a φX174 data set (Dokland *et al.*, 1997) processed by method 2. The observed partialities for individual partial reflections were averaged in bins of calculated partialities. The broken line represents the ideal relationship $p_{obs} = p_{calc}$.

11.5.7.3. *Statistics for rejecting reflections and data quality as a function of frame number*

The behaviour of the *R* factor *versus* frame number (Fig. 11.5.7.5) is more monotonic when method 1 is used compared to method 2. In method 1, the data-quality estimates for neighbouring frames are strongly correlated because the full reflections used in the statistics are obtained by summing partials from consecutive frames. By contrast, in method 2 every frame produces estimates of full reflection intensities independently of the neighbouring frames. Therefore, the *R* factors per frame calculated after scaling with method 2 truly represent the data quality for individual frames.

11.5.7.4. *Observed versus calculated partiality*

The relationship between observed and calculated partialities (Fig. 11.5.7.6) deviates from the ideal line $p_{obs} = p_{calc}$, especially for the smaller calculated partialities where $p_{obs} > p_{calc}$. This suggests errors in the measurements of p_{obs} or the calculations of p_{calc}. The latter may be improved by a post refinement of the orientation matrix and crystal mosaicity (Rossmann *et al.*, 1979).

11.5.7.5. *Anisotropic mosaicity*

Refinement of the effective mosaicity can show both the anisotropic nature of the crystal (Fig. 11.5.7.7) as well as the impact of radiation damage. The effective mosaicity is the convolution of the mosaic spread of the crystal, the beam divergence and the wavelength divergence of the incident X-ray beam. Hence, X-ray diffraction data collected at a synchrotron-radiation source necessitate the differentiation of the effective mosaicity in the horizontal and vertical planes. A more general approach is the introduction of six parameters reflecting the anisotropic effective mosaicity.

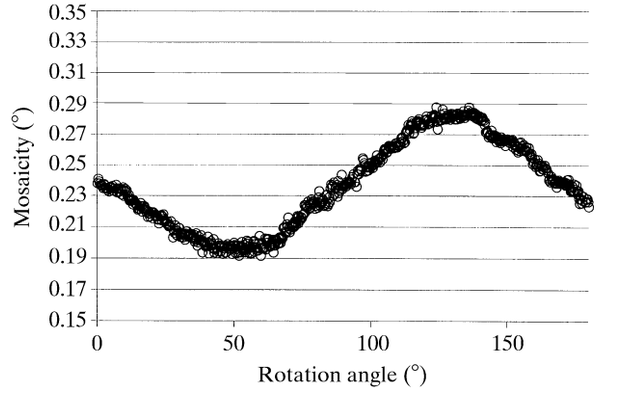

Fig. 11.5.7.7. Variation of (unconstrained) mosaicity for a monoclinic crystal of the bacterial virus alpha3 (Bernal *et al.*, 1998) showing the crystal anisotropy.

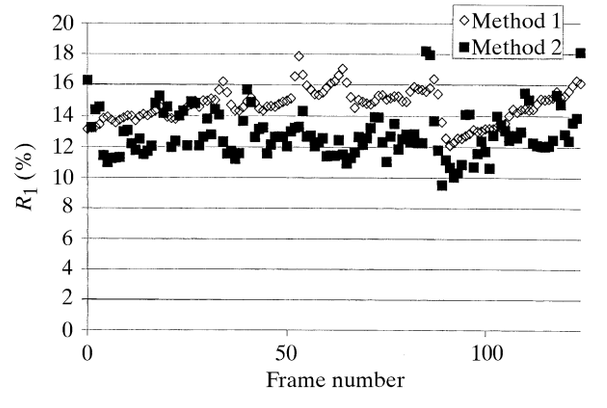

Fig. 11.5.7.5. *R* factor per frame as a function of frame number for a φX174 data set (Dokland *et al.*, 1997).

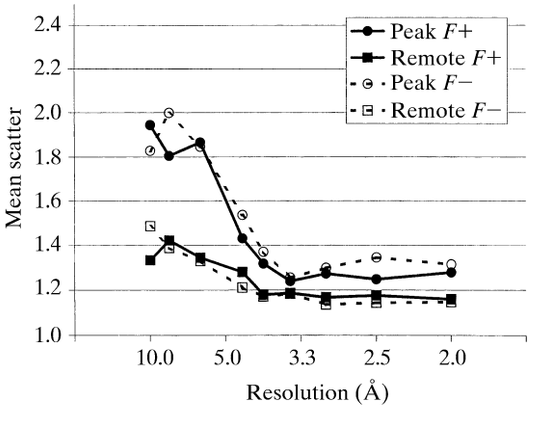

Fig. 11.5.7.8. Quality of anomalous-dispersion data for an SeMet derivative of dioxygenase Rieske ferredoxin (Colbert & Bolin, 1999).

11.5.7.6. *Anomalous dispersion*

The quality of anomalous-dispersion data can be assessed by calculation of the average scatter, expression (11.5.6.6). The ratios $\langle\sigma_{Ih}\rangle/\langle\sigma^{+}_{Ih}\rangle$ and $\langle\sigma_{Ih}\rangle/\langle\sigma^{-}_{Ih}\rangle$ should be larger than unity for significant anomalous data (Fig. 11.5.7.8). Note the much larger ratios for the scatter among measurements of I_h for data measured at the absorption edge of Se, as opposed to measurements remote from the edge. The decreasing values of the ratios with resolution are due to the decrease of I_h value, thus causing the error in the measurement of I_h to approach the difference in intensity of Bijvoet opposites.

11.5.8. Conclusions

The generalized HRS method allows scaling and averaging of X-ray diffraction data collected with an oscillation camera while simultaneously using full and partial reflections. The procedure is as useful for thin slices of reciprocal space as it is for thicker slices.

The results of data processing with the two different algorithms indicate that method 1, based on adding partial reflections, may fail to scale data sets with gaps in the rotation range or with low redundancy. The values of the scale factors obtained with both methods are similar, except for cases where there are gaps in the rotation range or dramatic changes in the true scale factors between consecutive frames. In these cases, method 1 produces a physically wrong result. The algorithm used by method 1 is probably similar to that used by *SCALEPACK* (Otwinowski & Minor, 1997).

Method 2 is more stable and versatile than method 1, and allows the scaling of data sets with incompletely measured reflections and low redundancy. The major drawback of method 2 is that errors in the crystal orientation matrix and mosaicity, as well as inadequacies of the theoretical model for reflection partiality, contribute to errors in the scaled intensities. Therefore, post refinement is needed for method 2 to perform at its best.

Appendix 11.5.1.

Partiality model (Rossmann, 1979; Rossmann *et al.*, 1979)

Small differences in the orientation of domains within the crystal, as well as the cross fire of the incident X-ray beam, will give rise to a series of possible Ewald spheres. Their extreme positions will subtend an angle $2m$ at the origin of the reciprocal space, and their centres lie on a cusp of limiting radius $\delta = m/\lambda$, where m is the half-angle effective mosaic spread. As the reciprocal lattice is rotated around the axis (Oy) perpendicular to the mean direction of the incident radiation (Oz), a point P will gradually penetrate the effective thickness of the reflection sphere (Fig. A11.5.1.1). Initially, only a few domain blocks will satisfy Bragg's law, but upon further rotation the number of blocks that are in a reflecting condition will increase. The maximum will be reached when the point P has penetrated halfway through the sphere's effective thickness, after which there will be a decline of the crystal volume able to diffract.

Let q be a measure of the fraction of the path travelled by P between the extreme reflecting positions P_A and P_B, and let p be the fraction of the energy already diffracted. Then the relation between p and q must have the general form shown in Fig. A11.5.1.2. It is physically reasonable to assume that the curve for p is tangential to $q = 0$ at $p = 0$ and to $q = 1$ at $p = 1$.

A reasonable approximation to the above conditions can be obtained by considering the fraction of the volume of a sphere removed by a plane a distance q from its surface (Fig. A11.5.1.2). It is easily shown that if p is the volume, then

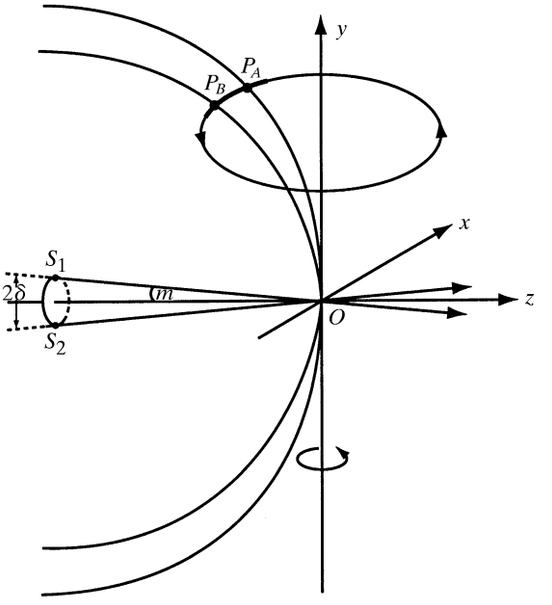

Fig. A11.5.1.1. Penetration of a reciprocal-lattice point P into the sphere of reflection by rotation around Oy. The extremes of reflecting conditions at P_A and P_B are equivalent to X-rays passing along the lines S_1O and S_2O with centres of the Ewald spheres at S_1 and S_2 and subtending an angle of $2m$ at O. Hence, in three dimensions, the extreme reflecting spheres will lie with their centres on a circle of radius $\delta = m/\lambda$ at $z = -1/\lambda$.

$$p = 3q^2 - 2q^3. \qquad \text{(A11.5.1.1)}$$

This curve is shown in Fig. A11.5.1.2 and corresponds to assuming that the reciprocal-lattice point is a sphere of finite volume cutting an infinitely thin Ewald sphere. Also shown in Fig. A11.5.1.2 is the line $p = q$ which would result if the reciprocal-lattice point were a rectangular block whose surfaces were parallel and perpendicular to the Ewald sphere at the point of penetration.

Assuming a right-handed coordinate system (x, y, z) in reciprocal space fixed to the camera, it is easily shown (Wonacott, 1977) that the condition for reflection is

$$d^{*2} + (2z/\lambda) = 0, \qquad \text{(A11.5.1.2)}$$

where d^* is the distance of a reciprocal-lattice point $P(x, y, z)$ from the origin, O, of reciprocal space. Similarly, it can be shown that at the ends of the path of the reciprocal-lattice point through the finite thickness of the sphere,

$$\begin{aligned} &d^{*2} + \delta^2 + (2z/\lambda) - 2\delta\left(x_A^2 + y_A^2\right)^{1/2} = 0 \quad \text{and} \\ &d^{*2} + \delta^2 + (2z/\lambda) - 2\delta\left(x_B^2 + y_B^2\right)^{1/2} = 0. \end{aligned} \qquad \text{(A11.5.1.3)}$$

Therefore,

$$\begin{aligned} z_A &= (\lambda/2)\left[-d^{*2} - \delta^2 + 2\delta\left(x_A^2 + y_A^2\right)^{1/2}\right], \\ z_B &= (\lambda/2)\left[-d^{*2} - \delta^2 + 2\delta\left(x_B^2 + y_B^2\right)^{1/2}\right]. \end{aligned} \qquad \text{(A11.5.1.4)}$$

Since δ is small, it can be assumed that $2\delta(x^2 + y^2)^{1/2}$ is independent of the position of the reciprocal-lattice point P between the extreme positions P_A and P_B (Fig. A11.5.1.1). Hence, the length of the path through the finite thickness of the sphere is proportional to

$$z_A - z_B = 2\lambda\delta\left(x_P^2 - y_P^2\right)^{1/2}. \qquad \text{(A11.5.1.5)}$$

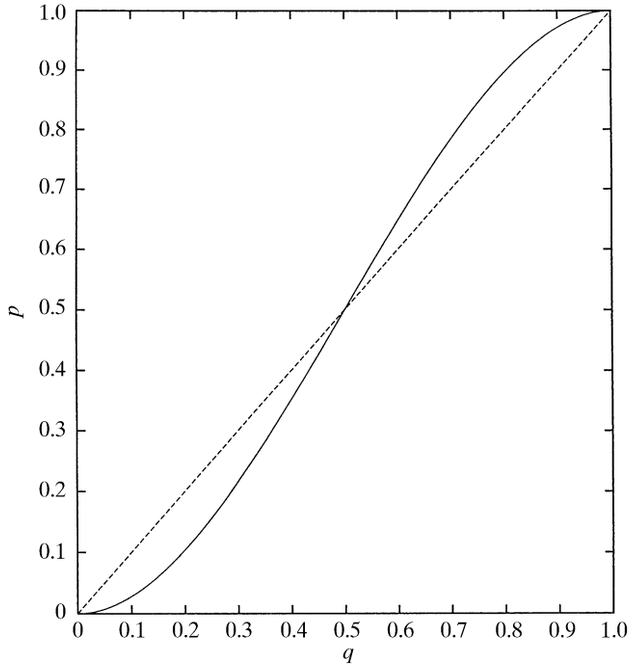

Fig. A11.5.1.2. Relationship between the fraction of the path travelled, q, by a reciprocal-lattice point across an Ewald sphere of finite thickness and the fraction of the total scattered intensity, p. The curve shown is for $p = 3q^2 - 2q^3$. As an extreme case, the line $p = q$ is also shown.

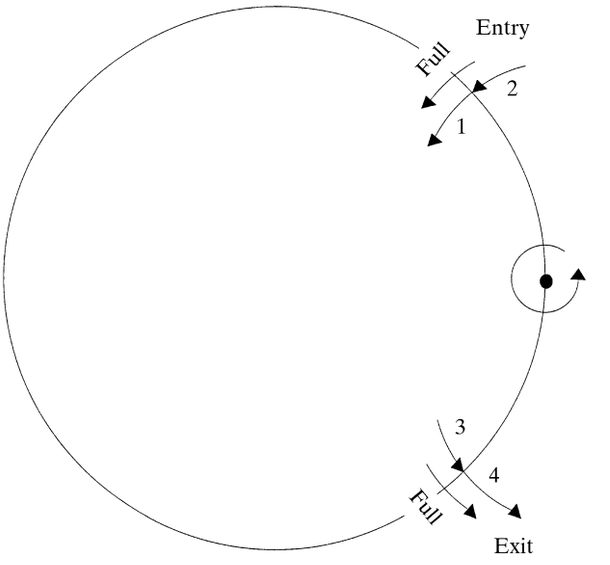

Fig. A11.5.1.3. The four conditions 1, 2, 3 and 4 for partial reflections corresponding to Table A11.5.1.1. The arrow ends and heads correspond to the start and end positions of a reciprocal-lattice point, respectively.

Now, if a reflection is only just penetrating the sphere at the end of the oscillation range, then the fraction of penetration is given by

$$q = PP_A/P_AP_B = (z_P - z_A)/(z_B - z_A). \qquad \text{(A11.5.1.6)}$$

Substituting this expression into equation (A11.5.1.4), it follows that

$$q = \tfrac{1}{2}[1 + (D_1/\eta_1)], \qquad \text{(A11.5.1.7)}$$

where

$$D = d^{*2} + \delta^2 + (2z/\lambda) \qquad \text{(A11.5.1.8)}$$

and

$$\eta = 2\delta(x^2 + y^2)^{1/2}. \qquad \text{(A11.5.1.9)}$$

The subscripts A and B refer to the beginning and end of the oscillation range for the partial reflection P, respectively.

Similarly, if a reflection is almost completely within the sphere,

$$q = PP_B/P_AP_B = (z_B - z_P)/(z_B - z_A) = \tfrac{1}{2}[1 - (D_2/\eta_2)]. \qquad \text{(A11.5.1.10)}$$

There are indeed four such conditions: two while a reflection is entering the Ewald sphere, and two while it is exiting. As such, it is readily seen that $-1 < (D_i/\eta_i) < 1$ ($i = 1$ or 2) is the range for a partial reflection. The full range of conditions is given in Table A11.5.1.1, as are the conditions for a full reflection.

Acknowledgements

This article is based primarily on the original publication by Bolotovsky *et al.* (1998). We are grateful for an NSF Grand Challenge grant in support of this work.

Table A11.5.1.1. *Calculation of the degree of penetration of the Ewald sphere, q*

The subscripts refer to the angles φ_1 and φ_2, designating the beginning and end of the oscillation range, respectively. See Fig. A11.5.1.3 for graphical representations of conditions 1 to 4.

	Almost completely within sphere	Almost completely outside sphere	Full reflection
Entering	Condition 1: $-1 < D_1/\eta_1 < +1$ and $D_2/\eta_2 \le -1$	Condition 2: $-1 < D_2/\eta_2 < +1$ and $D_1/\eta_1 \ge +1$	$D_1/\eta_1 \ge +1$ and $D_2/\eta_2 \le -1$
Exiting	Condition 3: $-1 < D_2/\eta_2 < +1$ and $D_1/\eta_1 \le -1$	Condition 4: $-1 < D_1/\eta_1 < +1$ and $D_2/\eta_2 \ge +1$	$D_1/\eta_1 \le -1$ and $D_2/\eta_2 \ge +1$

References

11.1

Bricogne, G. (1986). *Indexing and the Fourier transform.* In *Proceedings of the EEC cooperative workshop on position-sensitive detector software (phase III)*, p. 28. LURE, Paris, 12–19 November.

Burzlaff, H., Zimmermann, H. & de Wolff, P. M. (1992). *Crystal lattices*. In *International Tables for Crystallography*, Vol. A. *Space-group symmetry*, edited by T. Hahn. Dordrecht: Kluwer Academic Publishers.

Campbell, J. W. (1997). In *CCP4 Newsletter*, No. 33, edited by M. Winn. Warrington: Daresbury Laboratory.

Duisenberg, A. J. M. (1992). *Indexing in single-crystal diffractometry with an obstinate list of reflections. J. Appl. Cryst.* **25**, 92–96.

Higashi, T. (1990). *Auto-indexing of oscillation images. J. Appl. Cryst.* **23**, 253–257.

Kabsch, W. (1988). *Automatic indexing of rotation diffraction patterns. J. Appl. Cryst.* **21**, 67–71.

Kabsch, W. (1993). *Automatic processing of rotation diffraction data from crystals of initially unknown symmetry and cell constants. J. Appl. Cryst.* **26**, 795–800.

Kim, S. (1989). *Auto-indexing oscillation photographs. J. Appl. Cryst.* **22**, 53–60.

Leslie, A. G. W. (1992). *Recent changes to the MOSFLM package for processing film and image plate data.* In *CCP4 and ESF-EACMB Newsletter on Protein Crystallography*, No. 26. Warrington: Daresbury Laboratory.

Otwinowski, Z. & Minor, W. (1997). *Processing of X-ray diffraction data collected in oscillation mode. Methods Enzymol.* **276**, 307–326.

Rossmann, M. G. (1979). *Processing oscillation diffraction data for very large unit cells with an automatic convolution technique and profile fitting. J. Appl. Cryst.* **12**, 225–238.

Rossmann, M. G. & Erickson, J. W. (1983). *Oscillation photography of radiation-sensitive crystals using a synchrotron source. J. Appl. Cryst.* **16**, 629–636.

Sparks, R. A. (1976). *Trends in minicomputer hardware and software. Part I.* In *Crystallographic computing techniques*, edited by F. R. Ahmed, K. Huml & B. Sedláček, pp. 452–467. Copenhagen: Munksgaard.

Sparks, R. A. (1982). *Data collection with diffractometers.* In *Computational crystallography*, edited by D. Sayre, pp. 1–18. New York: Oxford University Press.

Steller, I., Bolotovsky, R. & Rossmann, M. G. (1997). *An algorithm for automatic indexing of oscillation images using Fourier analysis. J. Appl. Cryst.* **30**, 1036–1040.

Strouse, C. E. (1996). Personal communication.

Tao, Y., Strelkov, S. V., Mesyanzhinov, V. V. & Rossmann, M. G. (1997). *Structure of bacteriophage T4 fibritin: a segmented coiled coil and the role of the C-terminal domain. Structure*, **5**, 789–798.

Vriend, G. & Rossmann, M. G. (1987). *Determination of the orientation of a randomly placed crystal from a single oscillation photograph. J. Appl. Cryst.* **20**, 338–343.

Wonacott, A. J. (1977). *Geometry of the rotation method.* In *The rotation method in crystallography*, edited by U. W. Arndt & A. J. Wonacott, pp. 75–103. Amsterdam: North-Holland Publishing Co.

11.2

Diamond, R. (1969). *Profile analysis in single crystal diffractometry. Acta Cryst.* A**25**, 43–55.

Ford, G. C. (1974). *Intensity determination by profile fitting applied to precession photographs. J. Appl. Cryst.* **7**, 555–564.

Greenhough, T. J. & Suddath, F. L. (1986). *Oscillation camera data processing. 4. Results and recommendations for the processing of synchrotron radiation data in macromolecular crystallography. J. Appl. Cryst.* **19**, 400–409.

Lehmann, M. S. & Larsen, F. K. (1974). *A method for location of the peaks in step-scan-measured Bragg reflexions. Acta Cryst.* A**30**, 580–584.

Leslie, A. G. W. (1992). *Recent changes to the MOSFLM package for processing film and image plate data. CCP4 and ESF-EACMB Newsletter on Protein Crystallography*. Warrington: Daresbury Laboratory.

Otwinowski, Z. & Minor, W. (1997). *Processing of X-ray diffraction data collected in oscillation mode. Methods Enzymol.* **276**, 307–326.

Rossmann, M. G. (1979). *Processing oscillation diffraction data for very large unit cells with an automatic convolution technique and profile fitting. J. Appl. Cryst.* **12**, 225–238.

Rossmann, M. G., Leslie, A. G. W., Abdel-Meguid, S. S. & Tsukihara, T. (1979). *Processing and post-refinement of oscillation camera data. J. Appl. Cryst.* **12**, 570–581.

Winkler, F. K., Schutt, C. E. & Harrison, S. C. (1979). *The oscillation method for crystals with very large unit cells. Acta Cryst.* A**35**, 901–911.

11.3

Abramowitz, M. & Stegun, I. A. (1972). *Handbook of mathematical functions.* New York: Dover Publications.

Bricogne, G. (1986). *Indexing and the Fourier transform.* In *Proceedings of the EEC cooperative workshop on position-sensitive detector software (phase III)*, p. 28. LURE, 12–19 November.

Diamond, R. (1966). *A mathematical model-building procedure for proteins. Acta Cryst.* **21**, 253–266.

Diamond, R. (1969). *Profile analysis in single crystal diffractometry. Acta Cryst.* A**25**, 43–55.

Dijkstra, E. W. (1976). *A discipline of programming*, pp. 154–167. New Jersey: Prentice-Hall.

Ford, G. C. (1974). *Intensity determination by profile fitting applied to precession photographs. J. Appl. Cryst.* **7**, 555–564.

Fox, G. C. & Holmes, K. C. (1966). *An alternative method of solving the layer scaling equations of Hamilton, Rollett and Sparks. Acta Cryst.* **20**, 886–891.

Greenhough, T. J. & Helliwell, J. R. (1982). *Oscillation camera data processing: reflecting range and prediction of partiality. I. Conventional X-ray sources. J. Appl. Cryst.* **15**, 338–351.

Harrison, S. C., Winkler, F. K., Schutt, C. E. & Durbin, R. M. (1985). *Oscillation method with large unit cells. Methods Enzymol.* **114A**, 211–237.

Howard, A. (1986). *Autoindexing.* In *Proceedings of the EEC cooperative workshop on position-sensitive detector software (phases I & II)*, pp. 89–94. LURE, 26 May–7 June.

International Tables for Crystallography (1995). Vol. A. *Space-group symmetry*, edited by Th. Hahn, pp. 738–749. Dordrecht: Kluwer Academic Publishers.

Kabsch, W. (1988*a*). *Automatic indexing of rotation diffraction patterns. J. Appl. Cryst.* **21**, 67–71.

Kabsch, W. (1988*b*). *Evaluation of single-crystal X-ray diffraction data from a position-sensitive detector. J. Appl. Cryst.* **21**, 916–924.

Kabsch, W. (1993). *Automatic processing of rotation diffraction data from crystals of initially unknown symmetry and cell constants. J. Appl. Cryst.* **26**, 795–800.

Otwinowski, Z. (1993). *Oscillation data reduction program.* In *Proceedings of the CCP4 study weekend. Data collection and processing*, edited by L. Sawyer, N. Isaacs & S. Bailey, pp. 56–62. Warrington: Daresbury Laboratory.

Otwinowski, Z. & Minor, W. (1997). *Processing of X-ray diffraction data collected in oscillation mode. Methods Enzymol.* **276**, 307–326.

Pflugrath, J. W. (1997). *Diffraction-data processing for electronic detectors: theory and practice. Methods Enzymol.* **276A**, 286–306.

Rossmann, M. G. (1985). *Determining the intensity of Bragg reflections from oscillation photographs. Methods Enzymol.* **114A**, 237–280.

11.3 (*cont.*)

Schutt, C. & Winkler, F. K. (1977). *The oscillation method for very large unit cells.* In *The rotation method in crystallography*, edited by U. W. Arndt & A. J. Wonacott, pp. 173–186. Amsterdam, New York, Oxford: North-Holland.

Steller, I., Bolotovsky, R. & Rossmann, M. G. (1997). *An algorithm for automatic indexing of oscillation images using Fourier analysis. J. Appl. Cryst.* **30**, 1036–1040.

Wirth, N. (1976). *Algorithms + data structures = programs*, pp. 264–274. New York: Prentice-Hall.

11.4

Arndt, U. W. & Wonacott, A. J. (1977). *The rotation method in crystallography.* Amsterdam: North Holland.

Blessing, R. H. (1995). *An empirical correction for absorption anisotropy. Acta Cryst.* A**51**, 33–38.

Blum, M., Metcalf, P., Harrison, S. C. & Wiley, D. C. (1987). *A system for collection and on-line integration of X-ray diffraction data from a multiwire area detector. J. Appl. Cryst.* **20**, 235–242.

Bricogne, G. (1987). *The EEC cooperative programming workshop on position-sensitive detector software.* In *Proceedings of the Daresbury study weekend at Daresbury Laboratory*, 23–24 January, edited by J. R. Helliwell, P. A. Machin and M. Z. Papiz, pp. 120–146. Warrington: Daresbury Laboratory.

EEC Cooperative Workshop on Position-Sensitive Detector Software (1986). Phase I and II, LURE, Paris, 16 May–7 June; Phase III, LURE, Paris, 12–19 November.

Evans, P. (1993). *Data reduction: data collection and processing.* In *Proceedings of the CCP4 study weekend. Data collection and processing*, 29–30 January, edited by L. Sawyer, N. Isaac & S. Bailey, pp. 114–123. Warrington: Daresbury Laboratory.

Evans, P. R. (1987). *Postrefinement of oscillation camera data.* In *Proceedings of the Daresbury study weekend at Daresbury Laboratory*, 23–24 January, edited by J. R. Helliwell, P. A. Machin and M. Z. Papiz, pp. 58–66. Warrington: Daresbury Laboratory.

Fox, G. C. & Holmes, K. C. (1966). *An alternative method of solving the layer scaling equations of Hamilton, Rollett and Sparks. Acta Cryst.* **20**, 886–891.

Gewirth, D. (1996). *HKL manual.* 5th ed. Yale University, New Haven, USA.

Greenhough, A. G. W. (1987). *Partials and partiality.* In *Proceedings of the Daresbury study weekend at Daresbury Laboratory*, 23–24 January, edited by J. R. Helliwell, P. A. Machin and M. Z. Papiz, pp. 51–57. Warrington: Daresbury Laboratory.

Hammersley, A. P. (1998). *The FIT2D home page.* http://www.ccp14.ac.uk/ccp/web-mirrors/fit2d/computing/expg/subgroups/dataanalysis/FIT2D/index.html

Higashi, T. (1990). *Auto-indexing of oscillation images. J. Appl. Cryst.* **23**, 253–257.

Howard, A., Nielsen, C. & Xuong, Ng. H. (1985). *Software for a diffractometer with multiwire area detector. Methods Enzymol.* **114**, 452–472.

Howard, A. J., Gilliland, G. L., Finzel, B. C., Poulos, T. L., Ohlendorf, D. H. & Salemme, F. R. (1987). *The use of an imaging proportional counter in macromolecular crystallography. J. Appl. Cryst.* **20**, 383–387.

International Tables for Crystallography (1995). Vol. A. *Space-group symmetry*, edited by Th. Hahn. Dordrecht: Kluwer Academic Publishers.

Kabsch, W. (1988). *Evaluation of single-crystal X-ray diffraction data from a position sensitive detector. J. Appl. Cryst.* **21**, 916–924.

Kabsch, W. (1993). *Automatic processing of rotation diffraction data from crystals of initially unknown symmetry and cell constants. J. Appl. Cryst.* **26**, 795–800.

Katayama, C. (1986). *An analytical function for absorption correction. Acta Cryst.* A**42**, 19–23.

Kim, S. (1989). *Auto-indexing oscillation photographs. J. Appl. Cryst.* **22**, 53–60.

Leslie, A. (1993). *Autoindexing of rotation diffraction images and parameter refinement.* In *Proceedings of the CCP4 study weekend. Data collection and processing*, 29–30 January, edited by L. Sawyer, N. Isaac & S. Bailey, pp. 44–51. Warrington: Daresbury Laboratory.

Leslie, A. G. W. (1987). *Profile fitting.* In *Proceedings of the Daresbury study weekend at Daresbury Laboratory*, 23–24 January, edited by J. R. Helliwell, P. A. Machin and M. Z. Papiz, pp. 39–50. Warrington: Daresbury Laboratory.

Leslie, A. G. W. & Tsukihara, T. (1980). *A strategy for collecting isomorphous derivative data with the oscillation method. J. Appl. Cryst.* **13**, 304–305.

Messerschmidt, A. & Pflugrath, J. W. (1987). *Crystal orientation and X-ray pattern prediction routines for area-detector diffraction systems in macromolecular crystallography. J. Appl. Cryst.* **20**, 306–315.

Minor, W. & Otwinowski, Z. (1997). *Advances in accuracy and automation of data collection and processing.* In *Proceedings of the IUCr computing school*, Bellingham, 1996.

Naday, I., Ross, S., Westbrook, E. M. & Zentai, G. (1998). *Charge-coupled device/fiber optic taper array X-ray detector for protein crystallography. Opt. Eng.* **37**, 1235–1244.

Otwinowski, Z. (1993). *Oscillation data reduction program.* In *Proceedings of the Daresbury CCP4 study weekend. Data reduction and processing*, edited by L. Sawyer, N. Isaacs and S. Bailey, pp. 56–62. Warrington: Daresbury Laboratory.

Otwinowski, Z. & Minor, W. (1997). *Processing of X-ray diffraction data collected in oscillation mode. Methods Enzymol.* **276**, 307–326.

Press, W. H., Flannery, B. P., Teukolsky, S. A. & Vetterling, W. T. (1989). *Numerical recipes – the art of scientific computing.* Cambridge University Press.

Rossmann, M. G. (1979). *Processing oscillation diffraction data for very large unit cells with an automatic convolution technique and profile fitting. J. Appl. Cryst.* **12**, 225–238.

Rossmann, M. G. (1984). *Synchrotron radiation studies of large proteins and supramolecular structures.* In *Proceedings of the study weekend at Daresbury Laboratory. Biological systems: structure and analysis*, 24–25 March, edited by G. P. Diakun & C. D. Garner, pp. 28–40. Daresbury: Science and Engineering Research Council.

Rossmann, M. G. & Erickson, J. W. (1983). *Oscillation photography of radiation-sensitive crystals using a synchrotron source. J. Appl. Cryst.* **16**, 629–636.

Rossmann, M. G., Leslie, A. G. W., Abdel-Meguid, S. S. & Tsukihara, T. (1979). *Processing and post-refinement of oscillation camera data. J. Appl. Cryst.* **12**, 570–581.

Sakabe, N. (1991). *X-ray diffraction data collection system for modern protein crystallography with a Weissenberg camera and an imaging plate using synchrotron radiation. Nucl. Instrum. Methods A*, **303**, 448–463.

Schutt, C. E. & Evans, P. R. (1985). *Relative absorption correction for rotation film data. Acta Cryst.* A**41**, 568–570.

Schwarzenbach, D., Abrahams, S. C., Flack, H. D., Gonschorek, W., Hahn, Th., Huml, K., Marsh, R. E., Prince, E., Robertson, B. E., Rollett, J. S. & Wilson, A. J. C. (1989). *Statistical descriptors in crystallography. Acta Cryst.* A**45**, 63–75.

Steller, I., Bolotovsky, R. & Rossmann, M. G. (1997). *An algorithm for automatic indexing of oscillation images using Fourier analysis. J. Appl. Cryst.* **30**, 1036–1040.

Stuart, D. (1987). *Absorption correction.* In *Proceedings of the Daresbury study weekend at Daresbury Laboratory*, 23–24 January, edited by J. R. Helliwell, P. A. Machin & M. Z. Papiz, pp. 25–38. Warrington: Daresbury Laboratory.

Stuart, D. & Walker, N. (1979). *An empirical method for correcting rotation-camera data for absorption and decay effects. Acta Cryst.* A**35**, 925–933.

Takusagawa, F. (1987). *A simple method of absorption and decay correction in intensities measured by area-detector X-ray diffractometer. J. Appl. Cryst.* **20**, 243–245.

Tanaka, I., Yao, M., Suzuki, M., Hikichi, K., Matsumoto, T., Kozasa, M. & Katayama, C. (1990). *An automatic diffraction data*

collection system with an imaging plate. J. Appl. Cryst. **23**, 334–339.
Vriend, G. & Rossmann, M. G. (1987). *Determination of the orientation of a randomly placed crystal from a single oscillation photograph. J. Appl. Cryst.* **20**, 338–343.
Walker, N. & Stuart, D. (1983). *An empirical method for correcting diffractometer data for absorption effects. Acta Cryst.* A**35**, 158–166.
Winkler, F. K., Schutt, C. E. & Harrison, S. C. (1979). *The oscillation method for crystals with very large unit cells. Acta Cryst.* A**35**, 901–911.

11.5

Bernal, R., Burch, A., Fane, B. & Rossmann, M. G. (1998). Unpublished results.
Blessing, R. H. (1997). *Outlier treatment in data merging*. *J. Appl. Cryst.* **30**, 421–426.
Bolotovsky, R. & Coppens, P. (1997). *The φ extent of the reflection range in the oscillation method according to the mosaicity-cap model*. *J. Appl. Cryst.* **30**, 65–70.
Bolotovsky, R., Steller, I. & Rossmann, M. G. (1998). *The use of partial reflections for scaling and averaging X-ray area dectector data*. *J. Appl. Cryst.* **31**, 708–717.
Choi, H. K., Lee, S., Zhang, Y. P., McKinney, B. R., Wengler, G., Rossmann, M. G. & Kuhn, R. J. (1996). *Structural analysis of Sindbis virus capsid mutants involving assembly and catalysis*. *J. Mol. Biol.* **262**, 151–167.
Choi, H. K., Tong, L., Minor, W., Dumas, P., Boege, U., Rossmann, M. G. & Wengler, G. (1991). *Structure of Sindbis virus core protein reveals a chymotrypsin-like serine proteinase and the organization of the virion*. *Nature (London)*, **354**, 37–43.
Colbert, C. & Bolin, J. (1999). Unpublished results.
Dokland, T., McKenna, R., Ilag, L. L., Bowman, B. R., Incardona, N. L., Fane, B. A. & Rossmann, M. G. (1997). *Structure of a viral procapsid with molecular scaffolding*. *Nature (London)*, **389**, 308–313.
Fox, G. C. & Holmes, K. C. (1966). *An alternative method of solving the layer scaling equations of Hamilton, Rollett and Sparks*. *Acta Cryst.* **20**, 886–891.
Gewirth, D. (1996). *The HKL manual. A description of the programs DENZO, XDSPLAYF and SCALEPACK*, 5th ed., pp. 87–90. Yale University, New Haven, USA.
Greenhough, T. J. & Helliwell, J. R. (1982). *Oscillation camera data processing: reflecting range and prediction of partiality. I. Conventional X-ray sources*. *J. Appl. Cryst.* **15**, 338–351.
Hamilton, W. C., Rollett, J. S. & Sparks, R. A. (1965). *On the relative scaling of X-ray photographs*. *Acta Cryst.* **18**, 129–130.
Otwinowski, Z. & Minor, W. (1997). *Processing of X-ray diffraction data collected in oscillation mode*. *Methods Enzymol.* **276**, 307–326.
Rodgers, D. W. (1994). *Cryocrystallography*. *Structure*, **2**, 1135–1140.
Rossmann, M. G. (1979). *Processing oscillation diffraction data for very large unit cells with an automatic convolution technique and profile fitting*. *J. Appl. Cryst.* **12**, 225–238.
Rossmann, M. G., Arnold, E., Erickson, J. W., Frankenberger, E. A., Griffith, J. P., Hecht, H. J., Johnson, J. E., Kamer, G., Luo, M., Mosser, A. G., Rueckert, R. R., Sherry, B. & Vriend, G. (1985). *Structure of a human common cold virus and functional relationship to other picornaviruses*. *Nature (London)*, **317**, 145–153.
Rossmann, M. G., Leslie, A. G. W., Abdel-Meguid, S. S. & Tsukihara, T. (1979). *Processing and post-refinement of oscillation camera data*. *J. Appl. Cryst.* **12**, 570–581.
Rossmann, M. G., Momany, C. A., Cheng, B. & Chakravarty, S. (1997). Unpublished results.
Winkler, F. K., Schutt, C. E. & Harrison, S. C. (1979). *The oscillation method for crystals with very large unit cells*. *Acta Cryst.* A**35**, 901–911.
Wonacott, A. J. (1977). *Geometry of the oscillation method*. In *The rotation method in crystallography*, edited by U. W. Arndt & A. J. Wonacott, pp. 75–103. Amsterdam: North Holland.